Vacuum/volume 43/numbers 5–7/pages 381 to 385/1992
Printed in Great Britain

Pergamon Press Ltd

Characterization of fullerenes by laser-based mass spectrometry

Peter Wurz, Keith R Lykke, Michael J Pellin and Dieter M Gruen, *Materials Science/Chemistry Divisions, Argonne National Laboratory, Argonne, IL 60439, USA*

and

Deborah Holmes Parker, *Institute for Surface and Interface Science, University of California, Irvine, CA 92627, USA*

Mass characterization of C_{60} related high-mass carbon clusters, called fullerenes, and their compounds is of increasing interest as the unique properties of these materials become known. We are using laser desorption time-of-flight mass spectrometers to investigate direct emission of positive and negative ions and also neutral desorption. We show results on the laser desorption process, namely, desorption thresholds for positive ion, negative ion and neutral desorption and velocity distributions of desorbed neutral particles. Furthermore, post-ionization with the wavelengths 118, 212.8, 266, 355, and 532 nm is investigated.

1. Introduction

In laser vaporization experiments of graphite, large carbon clusters have been found under certain experimental conditions[1]. The most intense peak in the mass spectrum was identified as a cluster containing 60 carbon atoms and later was determined to have a truncated icosahedral structure[2], like a soccerball. The special stability of this cluster is related to the closed cage structure[3]. Similar carbon clusters, which all have an even number of atoms, exist from 32 atoms up to at least 400 atoms, with C_{60} the most stable one of this kind. This class of carbon clusters has been named 'fullerenes' after Buckminster Fuller, designer of the geodesic dome[4]. The recent development of a straightforward technique to synthesize and isolate C_{60} and higher mass fullerenes resulted in an enormous increase of research on these clusters in chemistry, physics, as well as in materials science. Recently, NMR spectra[5,6], uv/vis absorption data[5–7], ir emission[8] and ir absorption[7] spectra have been acquired for C_{60}, and the results support the icosahedral structure of the C_{60} molecule. By osmylating C_{60} it was possible to obtain X-ray diffraction data for this molecule, thus yielding experimental values for bond distances and bond angles in good agreement with theoretical predictions[9]. Using the Birch reduction, up to 36 hydrogen atoms could be attached onto a C_{60} cluster[10]. Furthermore, it was found that doping C_{60} with alkali metals not only turns this substance into a conductor[11], but the material also exhibits superconducting properties at temperatures well above the transition temperature for organic superconductors[12–18]. This can be regarded as a link between organic and inorganic superconductors.

Our work spans the generation, separation and mass spectroscopic characterization of these carbon clusters, including the synthesis of chemical compounds to photo-physical experiments with pure C_{60} as well as mixtures of fullerenes. Various A_xC_{60} compounds, with A being an alkali metal, have been synthesized by direct solution-phase chemical synthesis[13,16]. Characterization of the clusters and their compounds is carried out by utilizing either time-of-flight mass spectroscopy or high resolution Fourier transform mass spectroscopy. In these experiments, molecules are laser-desorbed from a substrate, and we detect either the directly emitted positive and negative ions or neutral species by post-ionization with intense laser light. This set-up also enables us to conduct photo-physical experiments with C_{60} and larger carbon clusters.

2. Mass spectrometry

A laser-desorption time-of-flight (TOF) mass spectrometer is used for the mass spectroscopic characterizations of fullerenes and fullerene-compounds. It has been discussed in detail previously[19], thus only a brief discussion is given here. The TOF mass spectrometer consists of an ion optics stack for acceleration, deflection plates, a field-free region and a dual channel plate assembly for the detection of ions. The apparatus can be operated in two modes: either measuring the mass spectrum of positive or negative ions emitted directly in the desorption process from the sample, or measuring the mass spectrum of desorbed neutrals by post-ionization with intense laser light. Potentials in the ion optics stack are optimized for best mass resolution in each mode. The instrument has a mass resolution ($m/\Delta m$) of up to 1500. The typical operating vacuum is $\approx 2 \times 10^{-9}$ torr. Samples are introduced by a rapid sample change port. Pulsed laser radiation is used to desorb neutral and ionized particles from a substrate coated with the sample material of interest. Subsequently, the desorbed neutral particles are ionized by a second pulsed laser. For a regular mass spectrum, the desorbed particles are ionized in close proximity to the sample surface (0.3 mm). To measure velocity distributions of desorbed neutral molecules, they are allowed to travel approximately 2 mm before being ionized in the acceleration field. By scanning the delay between the desorption and the ionization laser, a TOF spectrum of a particular molecule is obtained, which is subsequently converted to a velocity distribution. Mass spectroscopic data are recorded on a transient recorder with a maximum time resolution of 5 ns. Further processing of data is accomplished with a PC-based software system.

Either a XeCl excimer laser or the 2nd or 4th harmonic from a Q-switched Nd: YAG laser are used for laser desorption. The wavelength is chosen to provide good absorption of the radiation by the sample. Post-ionization is done in the wavelength range from 532 down to 118 nm (the 2nd to 9th harmonic from a second Nd: YAG laser). The experiment is operated at a 20 Hz repetition rate and the laser pulse widths are approximately 5 ns.

The relative timing of these lasers is controlled with a digital delay unit.

3. Preparation of fullerenes

For the production of macroscopic quantities of fullerenes it is necessary to evaporate graphite and collect the resulting soot which will cover the enclosing surfaces. The soot contains a certain amount of fullerenes when the evaporation is carried out in a helium atmosphere. This was first demonstrated by Krätschmer *et al* in early 1990[7]. Since then, two different methods for this synthesis have emerged: the evaporation method and the plasma method. In the evaporation method carbon is evaporated from graphite electrodes simply by resistively heating the electrodes[5,7,20]. When using the plasma method, carbon is evaporated by igniting a plasma between the graphite electrodes[6,10,21]. The latter method is more power-efficient and gives higher total yields of fullerenes[21]. Although every laboratory uses high purity graphite rods as the starting material for mass production of fullerenes, it has been demonstrated that fullerenes can also be generated from natural coal[22] or even from benzene flames[23], reducing the cost of production significantly.

We use the plasma method to synthesize the fullerenes. A dc-plasma is ignited between two graphite electrodes in a vacuum chamber filled with 200 torr helium after evacuating it with a mechanical pump. The resulting soot deposits on water-cooled collection surfaces, which surround the plasma region. After consuming several 1/4 in. electrodes, the vacuum chamber is backfilled to atmospheric pressure with helium and the soot is collected for further processing. Figure 1 shows a TOF mass spectrum of the raw soot, which has been deposited onto a stainless steel substrate in the graphite evaporator. The soot contains fullerenes from C_{60} up to C_{200}, and also low mass carbon clusters (size less than 32 atoms).

Fullerenes are removed from the soot by solvent extraction utilizing the Soxhlet technique. Figure 2 shows a negative ion mass spectrum from a toluene extract. Only carbon clusters consisting of 60 atoms or more are dissolved. The most abundant clusters are C_{60}, C_{70}, C_{78} and C_{84}. Furthermore, we observe a broad distribution of even numbered carbon clusters, which

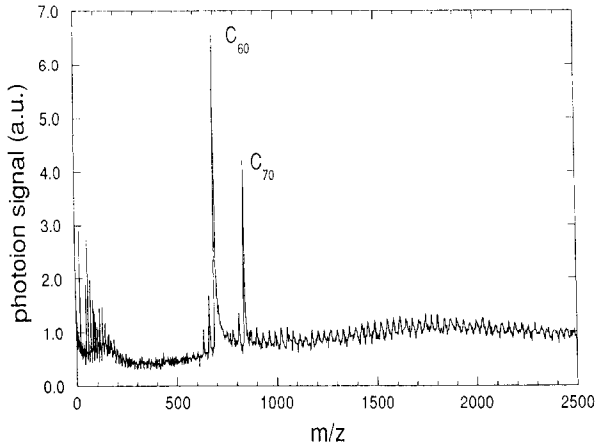

Figure 1. Laser desorption TOF mass spectrum of desorbed neutral particles from soot sample. A stainless steel substrate was placed in the graphite evaporation chamber and covered with soot before mass analysis. Post-ionization is performed with 212.8 nm light (5th harmonic of Nd : YAG laser).

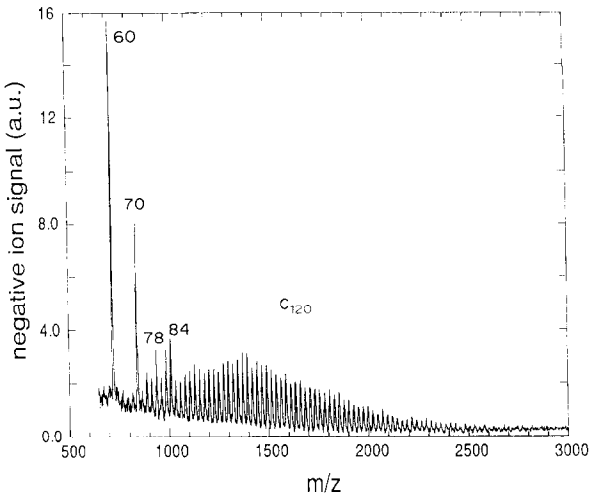

Figure 2. Laser desorption TOF mass spectrum of negative ions from raw toluene extract.

peaks around C_{120} and extends to clusters consisting of up to 200 atoms. No odd numbered carbon clusters are found. We have developed specialized multi-step extraction schemes[21], which are not only designed to achieve maximum yield of fullerenes from the soot, but also allow a preselection of molecular weight fractions of fullerenes. A different approach has been published recently using high pressure liquid chromatography for separation[24], which allows much narrower preselection of fullerenes, at limited mass range and quantities, however.

For the preparation of pure samples of C_{60} or C_{70}, we still have to resort to column chromatography. A toluene extract of fullerenes is placed on a chromatographic column of neutral alumina and hexane is used as the column eluent. The four panels in Figure 3 show TOF spectra from consecutive steps in the

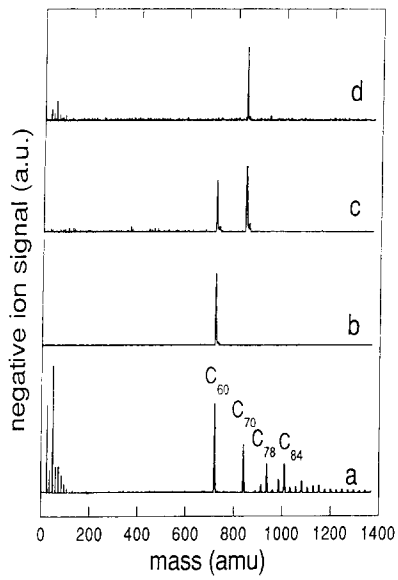

Figure 3. Laser desorption TOF negative ion mass spectra of raw toluene extract (a), first fraction off the chromatographic column (b), second fraction (c), and third fraction (d). In the raw extract the most abundant mass peaks are C_{60}, C_{70}, C_{78} and C_{84}, besides the low mass carbon clusters. C_{60} dominates in the first fraction, and C_{70} in the third; the second is a mixture of both.

separation sequence of C_{60} and C_{70} from the initial extract. These are laser desorption negative ion mass spectra, where a solution of material is put onto a stainless steel substrate with the solvent evaporated before introduction into the mass spectrometer. Panel (a) shows a mass spectrum of the toluene extract exhibiting a number of high mass peaks, with the clusters C_{60}, C_{70}, C_{78} and C_{84} being most abundant. Some low number carbon clusters are also present in the raw extract. In the first fraction coming off the chromatographic column (panel b) only C_{60} is detected. The second fraction (panel c) is a mixture of C_{60} and C_{70}, and finally the third fraction (panel d) consists almost entirely of C_{70}.

4. Laser desorption

As our mass spectroscopic instrument utilizes laser desorption to release sample material from a substrate into the vacuum, it was obvious to study laser desorption itself in some detail. In particular, the necessary laser fluences and the desorption thresholds are of great importance. Figure 4 shows the fluence thresholds for directly emitted positive and negative ions as well as the threshold for desorption of neutral C_{60} using 532 nm light for desorption. Post-ionization of desorbed neutrals is accomplished with 118 nm light to facilitate fragmentation-free ionization of the molecule (single-photon ionization). We find the thresholds for desorption at 1.6, 5.7 and 10.9 μJ mm^{-2} for neutral molecules and negative and positive ions, respectively. The difference in the desorption thresholds of neutral C_{60} molecules and C_{60} positive ions (almost a factor of 7) makes it possible to record mass spectra of desorbed neutrals free of interference from directly emitted positive ions without taking any further instrumental precautions. The structure of the signal dependence (neutrals, positive ions, negative ions) upon the laser fluence has little significance, as it strongly depends on the physical characteristics of the spot like homogeneity, laser absorbance and surface condition. In particular, the irradiation history of the spot from which desorption is obtained is of great importance. If the investigated spot was irradiated shortly before desorption (time scale of seconds), thresholds are found at much higher fluences, though the desorption site recovers after a while without irradiation. This explains why in laser desorption it is necessary to scan the laser over a small area to obtain a steady desorption signal.

In another set of measurements, we determined the velocity distributions for laser desorption of neutral C_{60} and C_{70} clusters from a stainless steel substrate[25]. Solutions of pure C_{60} or C_{70} are placed onto a polished stainless steel substrate and are inserted into the TOF spectrometer after solvent evaporation. The desorbed species are allowed to travel a short distance before being ionized and accelerated into the mass spectrometer. We kept the fluence of the desorption laser constant, a little above the threshold for direct ion production, to have sufficient neutral particle desorption. A gated integrator set at the arrival time of C_{60} or C_{70} is used for data acquisition, which further serves to eliminate interference from directly emitted ions. Several velocity distribution measurements for both samples are taken to ensure reproducibility. These velocity distributions are fitted with a Maxwell–Boltzmann distribution, giving good agreement with the measured data. Figure 5 shows a velocity distribution for each sample together with a best fit with a Maxwell–Boltzmann distribution. Theoretical calculations are performed to gauge the effect of angular and lateral distributions of the desorbed species on the measured velocity distribution for our particular set-up. We find that these have only a small effect compared with other uncertainties encountered in the measurement, although there is a systematic underestimation of the temperature of about 50 K. Taking this into account, we obtain average values for the temperatures of 2300 ± 200 and 1500 ± 100 K for the C_{60} and the C_{70} samples, respectively. This lets us favor a thermal process rather than the bond breaking mechanism as being responsible for laser desorption of C_{60} and C_{70} clusters, at the applied laser fluences. The physical principle of the bond breaking mechanism is that desorption is caused by excitation of an antibonding state of the parent or a fragment molecule[26], and thus fragmentation is expected in the desorption process. However, fragmentation is not observed in the desorption step under these laser fluences and is further evidence for thermal desorption (see Figure 3).

5. Photo-physics

Post-ionization of C_{60} by laser radiation at various harmonics of a Q-switched Nd : YAG-laser (118, 212.8, 266, 355, and 532 nm, corresponding to 10.5, 5.83, 4.66, 3.50 and 2.33 eV, respectively)

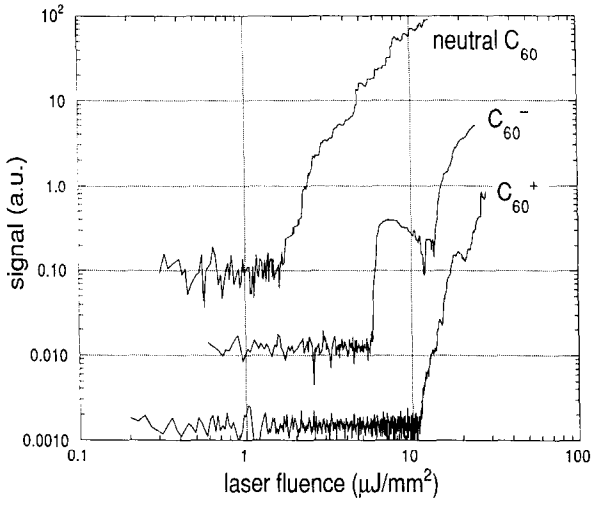

Figure 4. Laser (532 nm) fluence dependence of direct desorbed positive and negative C_{60} ions and neutral C_{60}, which is post-ionized with 118 nm light. The three curves have been offset vertically for clarity. The thresholds for desorption are found at 1.6, 5.7 and 10.9 μJ mm^{-2} for neutral molecules, negative and positive ions, respectively.

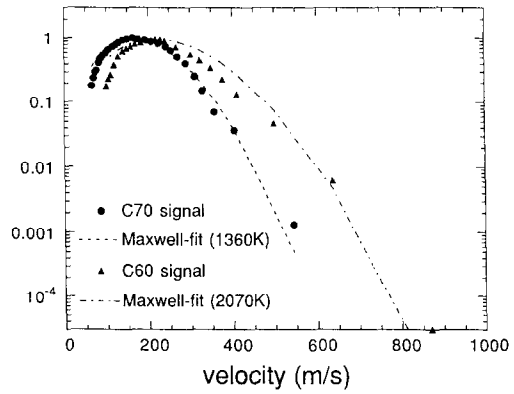

Figure 5. Velocity distributions for laser desorbed neutral C_{60} and C_{70}. Dashed curves give best fits of Maxwell–Boltzmann distributions with the measured data.

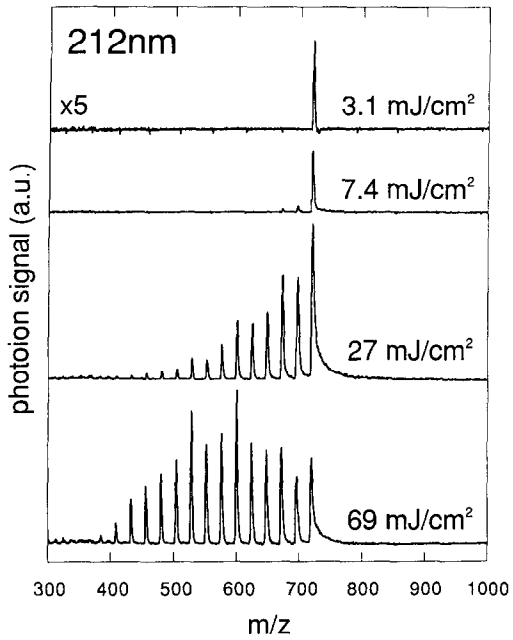

Figure 6. Laser ionization of C_{60} clusters from an effusive source by 212.8 nm light. The C_{60} parent ion and the even numbered fragment ions C_{58}, C_{56}, ... C_{32} are identified.

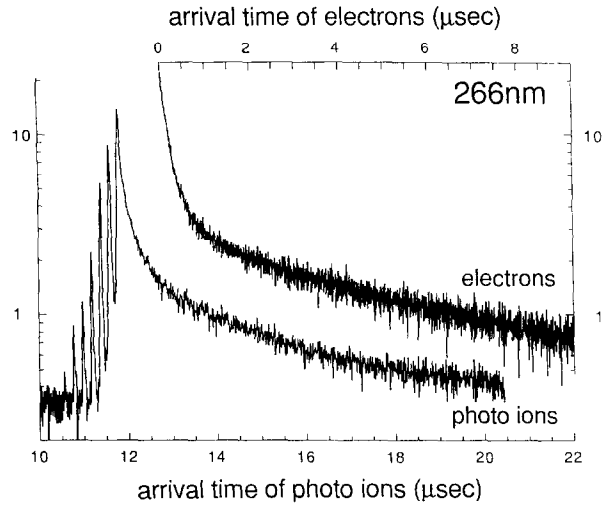

Figure 7. Time of arrival of photoelectrons and photoions for ionization of C_{60} with 266 nm laser light. The signal tails are identical for photoelectrons and photoions.

was investigated and will be presented in a forthcoming publication. A broad fluence range from the detection limit of the photoions to several orders of magnitude higher is covered. To overcome the limited signal stability inherent to laser desorption, we used an effusive source that provided a pure (99.9%) and stable C_{60} cluster beam. Figure 6 shows mass spectra of C_{60} at various laser fluences for post-ionization with 212.8 nm light. At very low laser fluences no fragmentation of C_{60} is observed. With rising laser fluence, fragmentation of the cluster is observed by loss of an even number of carbon atoms[25] and dominates the spectrum for high laser fluences. Using 266, 355 and 532 nm ionization always results in considerable fragmentation, even at very low laser fluences. For these wavelengths, we find similar fluence dependences, but shifted to higher fluence for longer wavelengths.

Careful observation of the mass spectra (Figure 6) shows that the parent mass peak is asymmetric (tailed) towards longer flight times. Furthermore, these tails exhibit the same fluence dependence as the fragmentation. The tails are attributed to thermionic emission of electrons from C_{60} molecules following multi-photon absorption[27]. Additional evidence for the observation of thermionic emission is the detection of the arrival time of the photoelectrons. A comparison of photoions and photoelectrons is depicted in Figure 7 for post-ionization with 266 nm light. We find *identical* tails for photoions and photoelectrons. In our apparatus, all photoelectrons produced are detected in the same way as photoions, by switching the polarity of the acceleration voltages (no electron energy dispersion). In the case of 212.8 nm light, the tails for photoions and photoelectrons both vanish if we go to very low laser fluences. However, this is merely an observation of limited detection sensitivity rather than a threshold for these processes. Fragmentation-free ionization without any delayed emission is observed only for 118 nm at all accessible laser fluences (see Figure 8). The absence of thermionic emission at 118 nm allows maximum mass resolution which enables us to resolve the isotope pattern of C_{60} ($m/\Delta m \approx 1500$).

6. Summary

We showed various steps in the sequence of generation and separation of fullerenes starting with evaporating graphite to soot, solvent extraction which allows for preselection of mass fractions of fullerenes complete separation of C_{60} and C_{70} by column chromatography. Laser desorption thresholds for direct emitted positive and negative C_{60} ions as well as neutral C_{60} molecules are presented. In addition velocity distributions of laser desorbed C_{60} and C_{70} favor a thermal desorption mechanism. In our laser desorption TOF mass spectroscopy studies, fragmentation-free desorption of fullerene molecules is easily achieved for direct emission of positive and negative ions as well

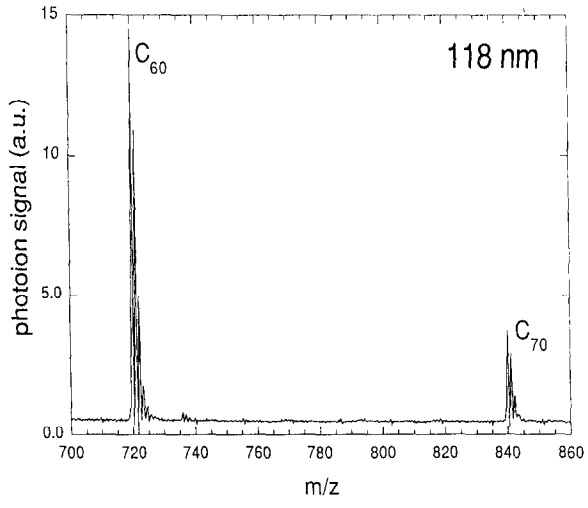

Figure 8. Time-of-flight mass spectrum of C_{60}/C_{70} mixture laser desorbed with 532 nm, post-ionized with 118 nm. Isotope distributions of C_{60} mass peak ($^{12}C_{60}$, $^{12}C_{59}{}^{13}C$, $^{12}C_{58}{}^{13}C_2$, ...) and of C_{70} mass peak ($^{12}C_{70}$, $^{12}C_{69}{}^{13}C$, $^{12}C_{68}{}^{13}C_2$, ...) are resolved. Masses 720 and 721 are separated by 25 ns.

as for neutral molecules with desorption lasers in the wavelength range from 266 to 532 nm. Unfortunately, post-ionization in this wavelength range results in considerable fragmentation of the parent molecules. Only 212.8 nm light at low laser fluences or 118 nm radiation allow fragmentation-free ionization, which is important for the mass spectroscopic analysis of fullerene compounds.

Acknowledgement

This work was supported by the US Department of Energy, BES-Materials Sciences, under Contract W-31-109-ENG-38.

References

[1] E A Rohlfing, D M Cox and A Kaldor, *J Chem Phys*, **81,** 3322 (1984).
[2] H W Kroto, J R Heath, S C O'Brien, R F Curl and R E Smalley, *Nature* **318,** 162 (1985).
[3] T G Schmalz, W A Seitz, D J Klein and G E Hite, *J Am Chem Soc*, **110,** 1113 (1988).
[4] H W Kroto, J R Heath, S C O'Brien, R F Curl and R E Smalley, *Nature*, **318,** 162 (1985).
[5] H Ajie, M Alvarez, S J Anz, R D Beck, F Diederich, K Fostiropoulos, D R Huffman, W Krätschmer, Y Rubin, K E Schriver, D Sensharma and R L Wetten, *J Phys Chem*, **94,** 8630 (1990).
[6] J P Hare, H W Kroto and R Taylor, *Chem Phys Lett*, **177,** 1394 (1991).
[7] W Krätschmer, L D Lamb, K Fostiropoulos and D R Huffman, *Nature*, **347,** 354 (1990).
[8] C J Frum, R Engelman Jr, H G Hedderich, P F Bernath, L D Lamb and D R Huffman, *Chem Phys Lett*, **176,** 504 (1991).
[9] J M Hawkins, A Meyer, T A Lewis, S Loren and F J Hollander, *Science*, **252,** 312 (1991).
[10] R E Haufler, J Conceicao, L P F Chibante, Y Chai, N E Byrne, S Flanagan, M M Haley, S C O'Brien, C Pan, Z Xiao, W E Billups, M A Ciufolini, R H Hauge, J L Margrave, L J Wilson, R F Curl and R E Smalley, *J Phys Chem*, **94,** 8634 (1990).
[11] R C Haddon, A F Hebard, M J Rosseinsky, D W Murphy, S J Duclos, K B Lyons, B Miller, J M Rosamilia, R M Fleming, A R Kortan, S H Glarum, A V Makhija, A J Muller, R H Eick, S M Zahurak, R Tycko, G Dabbagh and F A Thiel, *Nature*, **350,** 320 (1991).
[12] A F Hebard, M J Rosseinsky, R C Haddon, D W Murphy, S H Glarum, T T M Palstra, A P Ramirez and A R Kortan, *Nature*, **350,** 600 (1991).
[13] H H Wang, A M Kini, B M Savall, K D Carlson, J M Williams, K R Lykke, P Wurz, D H Parker, M J Pellin, D M Gruen, U Welp, W Kwok, S Fleshler and G W Crabtree, *Inorg Chem*, **30,** 2838 (1991).
[14] K Holczer, O Klein, S Huang, R B Kaner, K Fu, R L Wetten and F Diederich, *Science*, **252,** 1154 (1991).
[15] M J Rosseinsky, A P Ramirez, S H Glarum, D W Murphy, R C Haddon, A F Hebard, T T M Palstra, A R Kortan, S M Zahurak and A V Malchija, *Phys Rev Lett*, **66,** 2830 (1991).
[16] H H Wang, A M Kini, B M Savall, K D Carlson, J M Williams, M W Lathrop, K R Lykke, D H Parker, P Wurz, M J Pellin, D M Gruen, U Welp, W Kwok, S Fleshler, G W Crabtree, J E Schirber and D L Overmyer, *Inorg Chem*, **30,** 2962 (1991).
[17] K Tanigaki, T W Ebbesen, S Saito, J Mizuki, J S Tsai, Y Kubo and S Kuroshima, *Nature*, **352,** 222 (1991).
[18] S P Kelty, C Chen and C M Lieber, *Nature*, **352,** 223 (1991).
[19] J E Hunt, K R Lykke and M J Pellin, In *Methods and Mechanisms for Producing Ions from Large Molecules*. Plenum Press, Minaki (1991).
[20] R Taylor, J P Hare, A Abdul-Sada and H Kroto, *J Chem Soc Chem Commun*, 1423 (1990).
[21] D H Parker, P Wurz, K Chatterjee, K R Lykke, J E Hunt, M J Pellin, J C Hemminger, D M Gruen and L M Stock, *J Am Chem Soc*, **113,** 7499 (1991).
[22] L S K Pang, A M Vassallo and M A Wilson, *Nature*, **352,** 480 (1991).
[23] J B Howard, J T McKinnon, Y Makarovsky, A L Lafleur and M E Johnson, *Nature*, **352,** 139 (1991).
[24] F Diederich, R Ettl, Y Rubin, R L Wetten, R Beck, F Wudl, K C Khemani and A Koch, *Science*, **252,** 548 (1991).
[25] P Wurz, K R Lykke, M J Pellin and D M Gruen, *J Appl Phys*, **70,** 6647 (1991).
[26] S Lazare and V Granier, *Laser Chem*, **10,** 25 (1989).
[27] P Wurz and K R Lykke, *J Chem Phys*, **95,** 7008 (1991).